

increase. Since the  $\delta(^{13}\text{CO}_{\text{cis}})$  value for a given complex is less than the  $\delta(^{13}\text{CO}_{\text{trans}})$  value, the C atoms of the cis CO's are expected to be more susceptible to nucleophilic attack than is the C atom of the trans CO. Figure 4 shows plots of  $k_{\text{obsd}}$  vs  $\delta(^{13}\text{CO})$  for the reaction (eq 3). There is no correlation with  $\delta(^{13}\text{CO}_{\text{trans}})$ , and the correlation with  $\delta(^{13}\text{CO}_{\text{cis}})$  is not nearly as good as was obtained for a similar plot using the  $\nu_{\text{CO}}$  values (Figure 3). Yet the  $\delta(^{13}\text{CO})$  NMR results qualitatively support attack on a CO cis to L over the trans CO. Again, the  $\text{PPh}_3$  and  $\text{AsPh}_3$  derivatives react faster than expected on the basis of their  $\delta(^{13}\text{CO}_{\text{cis}})$  values (vide infra).

Since the rates of reaction of the  $\text{PPh}_3$  and the  $\text{AsPh}_3$  derivatives of  $\text{Mo}(\text{CO})_5\text{L}$  are much faster than expected on the basis of their  $A_1 \nu_{\text{CO}}$  bands and their  $\delta(^{13}\text{CO}_{\text{cis}})$  values, this suggests their rates of reaction, unlike the other ligands studied, are not controlled by electronic effects. One is then left with steric factors, and clearly the cone angles (Table V) of  $\text{PPh}_3$  and of  $\text{AsPh}_3$  are larger than for the other ligands used except for  $\text{P}(\text{c-Hx})_3$ . This greater bulk of the  $\text{PPh}_3$  or  $\text{AsPh}_3$  ligands may impose an enhanced cis effect on adjacent COs, rendering weaker M-C bonds both in the ground and in the transition states for reaction. Such a bond-weakening effect is supported by the small value of  $\Delta H^\ddagger$  of reaction for the reaction of  $\text{Mo}(\text{CO})_5\text{PPh}_3$  compared with the reaction of  $\text{Mo}(\text{CO})_5\text{P}(\text{OMe})_3$  (Table IV). Also the  $\text{PPh}_3$  system has a more negative  $\Delta S^\ddagger$  than does the  $\text{P}(\text{OMe})_3$  system, indicative of more steric strain for reaction. One drawback to this discussion is that the largest ligand  $\text{P}(\text{c-Hx})_3$  (Table V) system is then expected

to be the fastest to react, but it is found to be the slowest to react. It may be that this ligand, notorious for its huge size, has retarded an associative pathway for reaction sufficiently to just inadvertently give it a rate that seems to correlate the  $\nu_{\text{CO}}$  values (Figure 3). Clearly more detailed study and comprehension of steric and electronic factors influencing transition-metal-phosphorus(III) bonding are needed if we are to better understand experimental facts of the type reported here. For example, QALE<sup>18</sup> (quantitative analysis of ligand effects) is a recent attempt to quantify the heats of reaction of phosphorus ligands with organometallic compounds in terms of  $\sigma$ -electronic,  $\pi$ -electronic, and steric properties of the ligands.

**Acknowledgment.** We wish to thank the United States-China Cooperative Science Program for the support of this collaborative research. The program is under the auspices of the U.S. National Science Foundation and the PRC National Natural Science Foundation.

**Registry No.**  $\text{Mo}(\text{CO})_5\text{P}(\text{c-hx})_3$ , 15603-94-8;  $\text{Mo}(\text{CO})_5\text{P}(\text{n-Bu})_3$ , 15680-62-3;  $\text{Mo}(\text{CO})_5\text{NMe}_3$ , 15152-84-8;  $\text{Mo}(\text{CO})_5\text{py}$ , 14324-76-6;  $\text{Mo}(\text{CO})_5\text{PPh}_3$ , 14971-42-7;  $\text{Mo}(\text{CO})_5\text{AsPh}_3$ , 19212-22-7;  $\text{Mo}(\text{CO})_5\text{P}(\text{OEt})_3$ , 15603-75-5;  $\text{Mo}(\text{CO})_5\text{P}(\text{OMe})_3$ , 15631-20-6;  $\text{P}(\text{c-hx})_3$ , 2622-14-2;  $\text{P}(\text{n-Bu})_3$ , 998-40-3;  $\text{NMe}_3$ , 75-50-3;  $\text{py}$ , 110-86-1;  $\text{PPh}_3$ , 603-35-0;  $\text{AsPh}_3$ , 603-32-7;  $\text{P}(\text{OEt})_3$ , 122-52-1;  $\text{P}(\text{OMe})_3$ , 121-45-9;  $\text{Me}_3\text{NO}$ , 1184-78-7.

(18) Rahman, M. M.; Liu, H. Y.; Prock, A.; Giering, W. P. *Organometallics* 1987, 6, 650-658.

Contribution from the Department of Chemistry,  
University of Arizona, Tucson, Arizona 85721

## Destabilizing $d\pi$ - $p\pi$ Orbital Interactions and the Alkylation Reactions of Iron(II)-Thiolate Complexes<sup>1</sup>

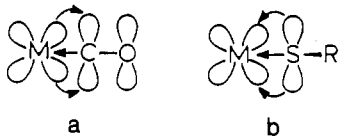
Michael T. Ashby, John H. Enemark,\* and Dennis L. Lichtenberger\*

Received November 19, 1986

For  $\text{CpFe}(\text{CO})_2\text{SR}$  (**1**) ( $\text{R} = \text{C}_6\text{H}_4\text{-}p\text{-Z}$ ;  $\text{Z} = \text{OMe}, \text{H}, \text{Cl}, \text{CF}_3, \text{NO}_2$ ) the  $\pi$ -type interaction between formally occupied metal d orbitals and the sulfur lone pair that is principally 3p in character has been modeled with Fenske-Hall molecular orbital calculations and experimentally investigated by gas-phase photoelectron spectroscopy. A calculation for **1** ( $\text{R} = \text{H}$ ) predicts that the highest occupied molecular orbital (HOMO) is metal-sulfur antibonding and largely sulfur in character. The observed HOMO ionization energies of **1** correlate with several chemical properties, including the rate of reaction of the thiolate ligand with alkyl halides. Solvent and substituent effects on the reaction rate favor a mechanism involving nucleophilic displacement of the halide by the coordinated thiolate ligand. The nucleophilicity of the coordinated thiolate ligand of **1** is related to the metal-sulfur  $d\pi$ - $p\pi$  antibonding interactions.

### Introduction

The Dewar-Chart-Duncanson model<sup>2</sup> has proven useful for rationalizing the stability of transition-metal complexes of  $\pi$ -acceptor ligands (e.g. carbon monoxide) and for explaining the



reactivity of such ligands (a). For example,  $\pi$ -acceptor ligands bound to transition metals in high oxidation states are generally more susceptible to nucleophilic attack than are  $\pi$ -acceptor ligands

bound to low-valent, electron-rich metals.<sup>3</sup> However,  $\pi$ -donor ligands have received much less attention. Thiolate ligands (b) possess a  $\sigma$ -donor orbital and a lone-pair orbital that is principally sulfur 3p in character. The latter orbital has the correct symmetry for  $\pi$  interactions with metal d orbitals.<sup>4</sup> If the metal d orbitals are formally occupied, the thiolate ligand may effectively serve as a four electron donor ( $2\sigma + 2\pi$ ). Recently, the stabilities of a highly oxidized transition-metal-carbonyl complex,  $\text{Ru}^{\text{IV}}(\text{S}-2,3,5,6\text{-Me}_4\text{C}_6\text{H})_4(\text{CO})$ ,<sup>5</sup> and of a coordinatively unsaturated

- (1) Presented in part in: Ashby, M. T.; Enemark, J. H.; Lichtenberger, D. L. *Abstracts*, XIIth International Conference on Organometallic Chemistry, Vienna, Austria, Sept. 1985; No. 503.  
(2) (a) Dewar, M. J. S. *Bull. Soc. Chim. Fr.* 1951, 18, C79. (b) Dewar, M. J. S. *Annu. Rep. Prog. Chem.* 1951, 48, 112. (c) Chatt, J.; Duncanson, L. A. *J. Chem. Soc.* 1953, 2339.

- (3) (a) Collman, J. P.; Hegedus, L. S. *Principles and Applications of Organotransition Metal Chemistry*; University Science Books: Mill Valley, CA, 1980; p 298. (b) Lukehart, C. M. *Fundamental Transition Metal Organometallic Chemistry*; Brooks/Cole: Monterey, CA, 1985; p 313. (c) Wong, D. K.; Madhavarac, M.; Marten, D. F.; Rosenblum, M. *J. Am. Chem. Soc.* 1977, 99, 2823.  
(4) (a) Lauher, J. W.; Hoffmann, R. *J. Am. Chem. Soc.* 1976, 98, 1729. (b) Kamata, M.; Hirotsu, K.; Higuchi, T.; Tasumi, K.; Hoffmann, R.; Yoshida, T.; Otsuka, S. *J. Am. Chem. Soc.* 1981, 103, 5772. (c) Kamata, M.; Yoshida, T.; Otsuka, S.; Hirotsu, K.; Higuchi, T.; Kito, M.; Tatsumi, K.; Hoffmann, R. *Organometallics* 1982, 1, 227. (d) Ashby, M. T.; Enemark, J. H. *J. Am. Chem. Soc.* 1986, 108, 730.

complex,  $\text{CpMo}(\text{NO})(\text{SC}_6\text{H}_5)_2$ ,<sup>4d</sup> have been attributed to  $\pi$  donation by the thiolate ligands.

In this paper we consider the  $d\pi$ - $p\pi$  antibonding interactions in the pseudooctahedral  $d^6$  complexes  $\text{CpFe}(\text{CO})_2\text{SR}$  (**1**), which have thiolate ligands bound to a transition metal in a relatively low oxidation state. The electronic structure of **1** has been modeled by using Fenske-Hall molecular orbital calculations and experimentally investigated by gas-phase photoelectron spectroscopy (PES). The reactivity of **1** with alkyl halides has also been studied, and the rate data are correlated with the spectroscopic data. This is the first detailed study of the relationship between metal-thiolate  $d\pi$ - $p\pi$  antibonding orbital interactions and the nucleophilicity of the coordinated thiolate ligand.

## Experimental Section

**Materials and Methods.** Solution manipulations were carried out under argon by using standard Schlenk techniques. Solvents were dried prior to use.<sup>5</sup> The  $^1\text{H}$  NMR spectra were obtained on  $\text{CDCl}_3$  solutions of the compounds on a Bruker WM-250. The chemical shifts are reported in  $\delta$  versus an internal standard of TMS. Infrared spectra were obtained on a Perkin-Elmer PE-983 instrument on  $\text{CHCl}_3$  solutions of the compounds between NaCl plates. All of the mercaptans were purchased from Aldrich and used as received except *p*-(trifluoromethyl)-benzenethiol, which was prepared according to Holm et al.<sup>7</sup> Cyclopentadienyliron dicarbonyl dimer was purchased from Strem.  $\text{CpFe}(\text{CO})_2\text{I}$ ,<sup>8</sup>  $\text{CpFe}(\text{CO})_2\text{SC}_2\text{H}_5$ ,<sup>9a</sup> and  $\text{CpFe}(\text{CO})_2\text{SC}_6\text{H}_5$ ,<sup>9a</sup> were prepared by published procedures.

**$\text{CpFe}(\text{CO})_2\text{SC}_6\text{H}_4$ -*p*-**Z**.** The para-substituted analogues of **1** ( $\text{R} = \text{C}_6\text{H}_4$ -*p*-**Z**; **Z** = OMe, H, Cl,  $\text{CF}_3$ ,  $\text{NO}_2$ ) may be prepared by a route similar to that used to prepare **1** ( $\text{R} = \text{C}_2\text{H}_5$  and  $\text{C}_6\text{H}_5$ ).<sup>9a</sup> Typically, the sodium salt of the mercaptan was prepared by treatment of the corresponding mercaptan with sodium hydride in dry THF under argon. One equivalent of  $\text{CpFe}(\text{CO})_2\text{I}$  was added as a solid, and the resulting solution was stirred for ca. 2 h. The solvent was removed with a rotary evaporator, and the resulting residue, extracted with a minimum amount of benzene, was chromatographed on neutral silica gel, eluting with benzene. Occasionally a light brown band of disulfide and unreacted  $\text{CpFe}(\text{CO})_2\text{I}$  was observed to elute followed closely by the product, which was generally collected as a single fraction. The benzene solution was reduced in volume with a rotary evaporator, and petroleum ether was added to precipitate the product as a solid except for **1** ( $\text{R} = \text{C}_6\text{H}_4$ -*p*-OMe), which could be obtained as crystals at  $-78^\circ\text{C}$  that melt upon warming to room temperature. The products were judged pure by IR and  $^1\text{H}$  NMR spectroscopy. For **1** ( $\text{R} = \text{C}_6\text{H}_4$ -*p*-OMe): yield = 58%; IR ( $\text{CHCl}_3$ ) 2032, 1984 (CO)  $\text{cm}^{-1}$ ;  $^1\text{H}$  NMR ( $\text{CDCl}_3$ )  $\delta$  7.46, 6.68 (AA'XX'),  $J_{\text{AX}} = J_{\text{AX}'} = 8.8$  Hz,  $J_{\text{AX}''} = J_{\text{AX}'''} = 2.2$  Hz, 4 H,  $-\text{C}_6\text{H}_4-$ , 4.89 (s, 5 H,  $\text{C}_6\text{H}_5$ ), 3.76 (s, 3 H,  $-\text{CH}_3$ ). For **1** ( $\text{R} = \text{C}_6\text{H}_4$ -*p*-Cl): yield = 68%; IR ( $\text{CHCl}_3$ ) 2036, 1989 (CO)  $\text{cm}^{-1}$ ;  $^1\text{H}$  NMR ( $\text{CDCl}_3$ )  $\delta$  7.42, 7.06 (AA'XX'),  $J_{\text{AX}} = J_{\text{AX}'} = 8.6$  Hz,  $J_{\text{AX}''} = J_{\text{AX}'''} = 2.0$  Hz, 4 H,  $-\text{C}_6\text{H}_4-$ , 4.94 (s, 5 H,  $\text{C}_6\text{H}_5$ ). For **1** ( $\text{R} = \text{C}_6\text{H}_4$ -*p*- $\text{CF}_3$ ): yield = 52%; IR ( $\text{CHCl}_3$ ) 2039, 1992 (CO)  $\text{cm}^{-1}$ ;  $^1\text{H}$  NMR ( $\text{CDCl}_3$ )  $\delta$  7.55, 7.32 (AX,  $J_{\text{AX}} = 7.5$  Hz, 4 H,  $-\text{C}_6\text{H}_4-$ ), 5.01 (s, 5 H,  $\text{C}_6\text{H}_5$ ). For **1** ( $\text{R} = \text{C}_6\text{H}_4$ -*p*- $\text{NO}_2$ ): yield = 57%; IR ( $\text{CHCl}_3$ ) 2043, 1997 (CO)  $\text{cm}^{-1}$ ;  $^1\text{H}$  NMR ( $\text{CDCl}_3$ )  $\delta$  7.93, 7.48 (AA'XX'),  $J_{\text{AX}} = J_{\text{AX}'} = 8.9$  Hz,  $J_{\text{AX}''} = J_{\text{AX}'''} = 2.0$  Hz, 4 H,  $-\text{C}_6\text{H}_4-$ , 5.10 (s, 5 H,  $\text{C}_6\text{H}_5$ ).

**6-Iodo-1-hexene.** The Finkelstein reaction was employed.<sup>10</sup> To a 50-mL Schlenk flask was added 6-bromo-1-hexene (1.0 g, 6.1 mmol), sodium iodide (3.0 g, 20.0 mmol), and 20 mL of acetone. The resulting slurry was refluxed for 36 h. The acetone was removed under vacuum, and the remaining residue was extracted with 20 mL of ether. The ether was evaporated, and the crude product was vacuum (flash) distilled to give 6-iodo-1-hexene as a colorless liquid in near quantitative yield and free of the corresponding bromide.  $^1\text{H}$  NMR ( $\text{DMSO}-d_6$ ):  $\delta$  5.74–5.85 (m, 1 H,  $=\text{CHR}$ ), 4.93–5.06 (m, 2 H,  $=\text{CH}_2$ ), 3.28 (t,  $J = 7.5$  Hz, 2 H,  $-\text{CH}_2$ ), 1.99–2.08 (m, 2 H,  $-\text{CH}_2$ ), 1.70–1.82 (m, 2 H,  $-\text{CH}_2$ ), 1.40–1.49 (m, 2 H,  $-\text{CH}_2$ ).

- (5) Millar, M. M.; O'Sullivan, T.; de Vries, M.; Koch, S. A. *J. Am. Chem. Soc.* **1985**, *107*, 3714.  
 (6) Perrin, D. D.; Armarego, W. L. F.; Perrin, D. R. *Purification of Laboratory Chemicals*; Pergamon: London, 1980.  
 (7) Wong, G. B.; Kurtz, D. M., Jr.; Holm, R. H.; Mortenson, L. E.; Upchurch, R. G. *J. Am. Chem. Soc.* **1979**, *101*, 3078.  
 (8) King, R. B.; Stone, F. G. A. *Inorg. Synth.* **1963**, *7*, 110.  
 (9) (a) Ahmad, M.; Bruce, R.; Knox, G. R. *J. Organomet. Chem.* **1966**, *6*, 1. (b) King, R. B.; Bisnette, M. B. *J. Am. Chem. Soc.* **1964**, *86*, 1267. (c) Dekker, M.; Knox, G. R.; Robertson, C. G. *J. Organomet. Chem.* **1969**, *18*, 161.  
 (10) Finkelstein, H. *Ber. Dtsch. Chem. Ges.* **1910**, *43*, 1528.

**Table I.** Kinetic Study Reaction Conditions

Z	[Z], mol L <sup>-1</sup>	RX	[RX], mol L <sup>-1</sup>	solvent	$k$ , <sup>a</sup> L mol <sup>-1</sup> s <sup>-1</sup>
OMe	0.05	ICH <sub>3</sub>	0.25	acetone- <i>d</i> <sub>6</sub>	6.8 (4) × 10 <sup>-3</sup>
H	0.05	ICH <sub>3</sub>	0.56	acetone- <i>d</i> <sub>6</sub>	1.55 (3) × 10 <sup>-3</sup>
Cl	0.05	ICH <sub>3</sub>	0.56	acetone- <i>d</i> <sub>6</sub>	6.5 (3) × 10 <sup>-4</sup>
CF <sub>3</sub>	0.05	ICH <sub>3</sub>	0.25	acetone- <i>d</i> <sub>6</sub>	3.65 (13) × 10 <sup>-4</sup>
NO <sub>2</sub>	0.05	ICH <sub>3</sub>	0.56	acetone- <i>d</i> <sub>6</sub>	6.3 (4) × 10 <sup>-5</sup>
H	0.05	ICH <sub>2</sub> CH <sub>3</sub>	0.50	acetone- <i>d</i> <sub>6</sub>	8.6 (2) × 10 <sup>-5</sup>
H	0.05	ICH(CH <sub>3</sub> ) <sub>2</sub>	4.00	acetone- <i>d</i> <sub>6</sub>	no reaction
H	0.05	IC(CH <sub>3</sub> ) <sub>3</sub>	4.00	acetone- <i>d</i> <sub>6</sub>	no reaction
H	0.05	ICH <sub>3</sub>	0.10	dimethyl- <i>d</i> <sub>6</sub> sulfoxide	1.65 (4) × 10 <sup>-2</sup>
H	0.05	ICH <sub>3</sub>	0.50	chloroform- <i>d</i> <sub>1</sub>	1.37 (4) × 10 <sup>-3</sup>

<sup>a</sup> At 20 °C.

**Molecular Orbital Calculations.** Orbital eigenvalues were calculated by the Fenske-Hall self-consistent-field (SCF) method.<sup>11</sup> Atomic basis functions of Richardson<sup>12</sup> were used for iron (with a 4s exponent of 2.0 and a 4p exponent of 1.6) and Clementi<sup>13</sup> for carbon, oxygen (both with double- $\zeta$  functions with the 1s and 2s reduced to single- $\zeta$  form), and sulfur (with double- $\zeta$  functions with the 1s, 2s, 2p, and 3s reduced to a single- $\zeta$  form). An exponent of 1.2 was used for the hydrogen atom. Optimized bond lengths and angles were obtained from the X-ray crystal structure determination of **1** ( $\text{R} = \text{C}_2\text{H}_5$ ).<sup>14</sup> The geometry of the  $\text{CpFe}(\text{CO})_2$  fragment was the same as previously used.<sup>15a</sup> To simplify the calculations, the alkyl group bound to the sulfur was replaced with a hydrogen atom. An Fe-S bond length of 2.30 Å, S-H bond length of 1.35 Å, and a Fe-S-H bond angle of 107° were used. The angle is the average M-S-R angle for 16 reported structures of metal complexes of thiolates that possess primary R groups.<sup>16</sup> Calculations with an Fe-S-H angle of 120° were not significantly different.<sup>16</sup>

**Photoelectron Spectroscopy.** PES data were recorded on an instrument with a 36-cm radius hemispherical analyzer and a He I excitation source and data collection methods that have been described elsewhere.<sup>17</sup> It was necessary to heat the sample cell to obtain sufficient sample pressures. The temperature ranged from ca. 80 °C for **1** ( $\text{R} = \text{C}_6\text{H}_5$ ) to ca. 125 °C for **1** ( $\text{R} = \text{C}_6\text{H}_4$ -*p*- $\text{NO}_2$ ). A PES spectrum for **1** ( $\text{R} = \text{C}_6\text{H}_4$ -*p*-OMe) could not be obtained because the sample decomposed in the instrument. The argon ionization at 15.759 eV was used as an internal reference and lock of the energy scale. The energy scale did not drift more than 0.003 eV during data collection. The data were intensity corrected with an experimentally determined analyzer transmission function. The methods for curve-fit analysis have been previously described.<sup>17b,d</sup>

**Kinetic Studies.** A preliminary kinetic study of **1** ( $\text{R} = \text{C}_6\text{H}_5$ ) showed its reaction with iodomethane to be first order in each of the reactants and second order overall. In a typical experiment 0.5 mL of a 0.50 M solution of iodoalkane was added to 0.5 mL of a 0.10 M solution of **1**. After the two reactants were mixed, the resulting solution (0.25 M in iodoalkane and 0.05 M in **1**) was transferred to an NMR tube. The concentration of **1** was often limited to its solubility in the given solvent. The concentration of iodoalkane was chosen to give a reaction rate that could be conveniently followed by  $^1\text{H}$  NMR. The concentration of **1** was monitored as a function of time. Occasionally some of the ionic product **2** was observed to precipitate from the reaction mixture. Also, during a few experiments, small quantities of  $\text{CpFe}(\text{CO})_2\text{I}$  were observed to form. An internal standard of dichloromethane was used to insure the accurate integration of **1**. All of the products remained in solution when dimethyl-*d*<sub>6</sub> sulfoxide was used so an internal standard was unnecessary.

- (11) (a) Hall, M. B.; Fenske, R. F. *Inorg. Chem.* **1971**, *11*, 768. (b) Fenske, R. F. *Pure Appl. Chem.* **1971**, *27*, 61.  
 (12) Richardson, J. W.; Nieuport, W. C.; Powell, R. R.; Edgell, W. E. *J. Chem. Phys.* **1962**, *36*, 1057.  
 (13) Clementi, E. *J. Chem. Phys.* **1964**, *40*, 1944.  
 (14) English, R. B.; Nassimbeni, R.; Haines, R. J. *J. Chem. Soc., Dalton Trans.* **1978**, 1379.  
 (15) (a) Schilling, B. E. R.; Hoffmann, R.; Lichtenberger, D. L. *J. Am. Chem. Soc.* **1979**, *101*, 585. (b) Calabro, D. C.; Lichtenberger, D. L. *J. Am. Chem. Soc.* **1981**, *103*, 6846.  
 (16) Ashby, M. T. Ph.D. Dissertation, University of Arizona, 1986.  
 (17) (a) Calabro, D. C.; Hubbard, J. L.; Blevins, C. H., II; Cambell, A. C.; Lichtenberger, D. L. *J. Am. Chem. Soc.* **1981**, *103*, 6839. (b) Lichtenberger, D. L.; Calabro, D. C.; Kellogg, G. E. *Organometallics* **1984**, *3*, 1623. (c) Hubbard, J. L. Ph.D. Dissertation, University of Arizona, 1983. (d) Kellogg, G. E. Ph.D. Dissertation, University of Arizona, 1985. (e) Lichtenberger, D. L.; Kellogg, G. E.; Kristofzski, J. G.; Page, D.; Turner, S.; Klinger, G.; Lorenzen, J. *Rev. Sci. Instrum.* **1986**, *57*, 2366.

The experimental conditions for each of the kinetic experiments are given in Table I. Rate constants and their estimated standard deviation were obtained by a least-squares fit of the data.<sup>18f</sup> The rate constants from replicate experiments were reproducible within two estimated standard deviations.

**Mechanistic Studies. Attempts To Detect Radical Species by EPR.** To a  $\text{CCl}_4$  solution of **1** ( $\text{R} = \text{C}_6\text{H}_5$ ) (0.05 M) and 2-methyl-2-nitroso-propane (0.05 M) was added an excess quantity of iodomethane. After the resulting solution was allowed to react for a few minutes, a sample was removed and frozen in an EPR tube. An EPR signal was not observed for the frozen solution.

**Reaction of  $\text{CpFe}(\text{CO})_2\text{SC}_2\text{H}_5$  and 6-Iodo-1-hexene.** To a  $\text{DMSO}-d_6$  solution of **1** ( $\text{R} = \text{C}_2\text{H}_5$ ) [ $^1\text{H NMR}$  ( $\text{DMSO}-d_6$ )  $\delta$  5.21 (s, 5 H, Cp), 2.01 (q,  $J = 7.3$  Hz, 2 H,  $\text{CH}_2$ ), 1.12 (t,  $J = 7.3$  Hz, 3 H,  $\text{CH}_3$ )] was added 1 equiv of 6-iodo-1-hexene. The reaction was followed by  $^1\text{H NMR}$  spectroscopy. A transitory spectrum of **2** ( $\text{R} = \text{C}_2\text{H}_5$ ,  $\text{R}' = (\text{CH}_2)_4\text{CH}=\text{CH}_2$ ) [ $^1\text{H NMR}$  ( $\text{DMSO}-d_6$ )  $\delta$  5.72 (s, 5 H, Cp), 1.4–2.0 (unresolved peaks), 1.25 (t,  $J = 7.3$  Hz, 3 H,  $\text{CH}_3$ )] was slowly replaced with a spectrum of  $\text{CpFe}(\text{CO})_2\text{I}$  [ $^1\text{H NMR}$  ( $\text{DMSO}-d_6$ )  $\delta$  5.37 (s, 5 H, Cp)] and free 6-(ethylthio)-1-hexene [ $^1\text{H NMR}$  ( $\text{DMSO}-d_6$ )  $\delta$  5.53–5.81 (m, 1 H,  $=\text{CHR}$ ), 4.93–5.21 (m, 2 H,  $=\text{CH}_2$ ), 2.44–2.53 (m, 4 H,  $\text{RCH}_2\text{SCH}_2\text{R}' + \text{DMSO}$ ), 1.99–2.07 (m, 2 H,  $=\text{CH}_2$ ), 1.40–1.54 (m, 4 H,  $4-\text{CH}_2 + 5-\text{CH}_2$ ), 1.16 (t,  $J = 7.5$  Hz, 3 H,  $\text{CH}_3$ )]. No cyclic product was observed.

## Results and Discussion

**Molecular Orbital Calculations.** The pseudooctahedral geometry of **1** and its formal  $d^6$  electron configuration provide ideal molecular and electronic characteristics<sup>15</sup> to observe the effect of filled-filled  $d\pi-p\pi$  antibonding interactions between formally occupied metal orbitals and the thiolate ligand lone pair that is principally sulfur 3p in character. Fenske-Hall molecular orbital calculations were carried out in order to obtain a more detailed description of the electronic structure of **1** (see Experimental Section for details). To simplify the calculations, the alkyl group bound to the sulfur was replaced by a hydrogen atom. The coordinate system was chosen to be identical with that used in the previous theoretical treatment of  $\text{CpM}(\text{CO})_2\text{L}$  complexes.<sup>15</sup> The carbonyl ligands lie in the  $xy$  plane of the metal, and the  $y$  axis of the metal bisects the  $\text{OC}-\text{Fe}-\text{CO}$  angle. The thiolate sulfur atom is located on the  $z$  axis of the metal with the local  $z'$  coordinate of the sulfur pointed at its hydrogen atom. The local  $y'$  axis of the sulfur atom is in the  $\text{Fe}-\text{S}-\text{H}$  plane as shown in structure c, such that the sulfur  $x'$  axis is perpendicular to the metal  $z$  axis. The  $\text{Fe}-\text{S}-\text{H}$  angle is  $107^\circ$ .<sup>16</sup>



The bonding for **1** ( $\text{R} = \text{H}$ ) is conveniently described in terms of the molecular orbitals of the  $\text{CpFe}(\text{CO})_2^+$  and  $\text{SH}^-$  fragments. The relative energies of the significant orbitals of the  $\text{CpFe}(\text{CO})_2^+$  and  $\text{SH}^-$  fragments in  $\text{CpFe}(\text{CO})_2\text{SH}$  are shown in Figure 1a (left and right, respectively). The  $\text{S}-\text{H}$  bond ( $-15.8$  eV) and the sulfur  $3s-3p_z$  lone pair ( $-26.0$  eV) are too stable to include in the diagram. The HOMO's of the  $\text{SH}^-$  fragment are the sulfur  $3p_x$  and  $3p_y$  lone pairs and are designated the  $e'$  set ( $-10.6$  eV). Because of the stability and high sulfur 3s content of the sulfur  $3s-3p_z$  lone pair, the  $\sigma$ -bond formation of the sulfur to the metal is primarily from the  $3p_y$  component of the  $e'$  set of the  $\text{SH}^-$ , which  $\sigma$  donates

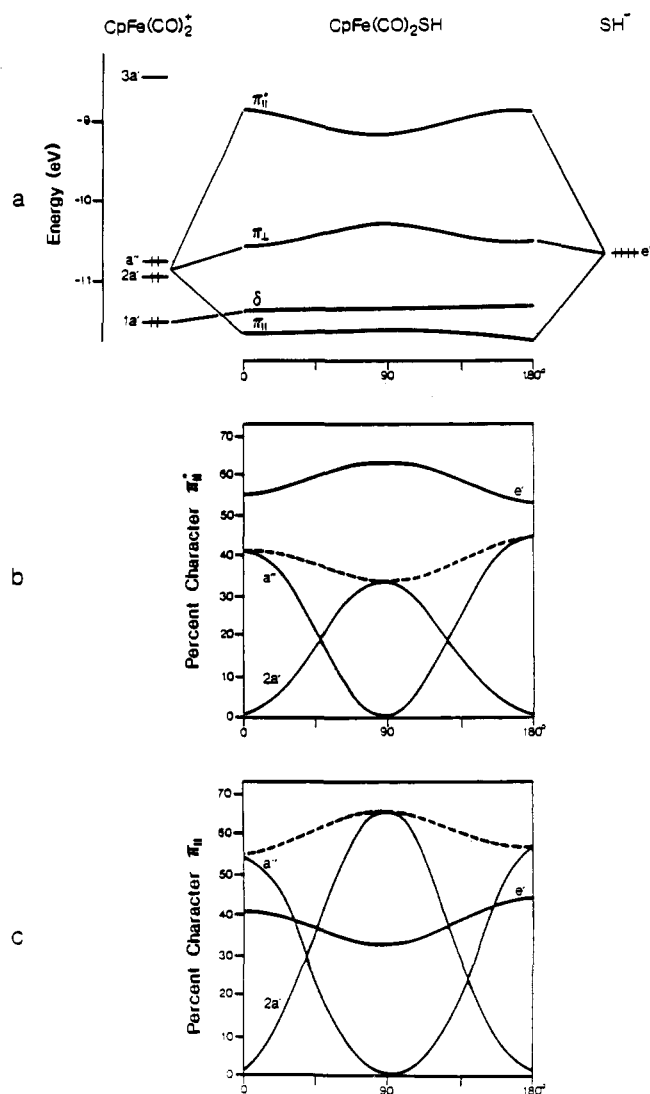
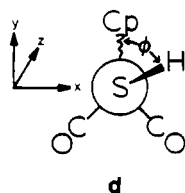


**Figure 1.** (a) Molecular orbital energy level diagram for  $\text{CpFe}(\text{CO})_2\text{SH}$ , showing the interaction of the frontier orbitals of the  $\text{CpFe}(\text{CO})_2^+$  fragment with the filled 3p orbitals of the  $\text{SH}^-$  fragment as a function of  $\phi$ , the rotational orientation of the coordinated  $\text{SH}^-$  group as shown in structure d. The HOMO ( $\pi^*$ ) is destabilized by the filled-filled  $d\pi-p\pi$  interaction. The  $\sigma_{\text{Fe-S}}$  ( $-12.4$  eV) and  $\sigma_{\text{Fe-S}}^*$  ( $1.6$  eV) levels are not shown, but both are relatively insensitive to  $\phi$ . (b) Percent character of the  $\pi^*$  orbital (HOMO) as a function of  $\phi$ . The orbital is principally sulfur 3p ( $e'$ ). The dashed line is the sum of the contributions from the  $2a'$  and  $a''$  orbitals of the  $\text{CpFe}(\text{CO})_2^+$  fragment. (c) Percent character of the  $\pi$  orbital as a function of  $\phi$ . The orbital is principally Fe 3d; the dashed line is the sum of the contributions of the  $2a'$  and  $a''$  orbitals of the  $\text{CpFe}(\text{CO})_2^+$  fragment.

to the empty  $3a'$  orbital of the  $\text{CpFe}(\text{CO})_2^+$  fragment;  $3a'$  is primarily of  $3d_{z^2}$  and  $4p_z$  character. The  $\sigma_{\text{Fe-S}}$  ( $-12.4$  eV) and  $\sigma_{\text{Fe-S}}^*$  ( $1.6$  eV) orbitals are not illustrated in Figure 1a, but both MO's are relatively insensitive to  $\phi$  (vide infra).

The  $\text{FeCp}(\text{CO})_2^+$  fragment can be regarded as a conventional pseudooctahedral complex with one ligand removed. The three highest occupied orbitals of the  $\text{CpFe}(\text{CO})_2^+$  fragment,  $1a'$ ,  $2a'$ , and  $a''$ , are related to the standard  $t_{2g}$  set of an octahedral  $d^6$  metal center. The  $1a'$  orbital of  $\text{CpFe}(\text{CO})_2^+$  from these calculations is primarily  $3d_{x^2-y^2}$  with some  $3d_{z^2}$  and  $3d_{yz}$ . It has predominantly  $\delta$  symmetry relative to the  $\text{SH}^-$  fragment and does not play a major role in  $\text{Fe}-\text{S}$  bonding. The  $2a'$  and  $a''$  orbitals both possess approximate  $\pi$  symmetry with respect to the sulfur atom and both are of the appropriate energy to mix with the sulfur  $3p_x$  member of the  $\text{SH}^-$  fragment. The nature of this  $\text{Fe}-\text{S}$   $d\pi-p\pi$  orbital interaction will depend upon the rotational orientation of the  $\text{SH}^-$  fragment, which is conveniently defined by  $\phi$ , the  $\text{H}-\text{S}-\text{Fe}-\text{Cp}$  (centroid) torsion angle (structure d).

- (18) (a) Petillon, F. Y.; LeFloch-Perrennou, F.; Guerchais, J. E.; Sharp, D. W. A. *J. Organomet. Chem.* **1979**, *173*, 89. (b) Guerchais, J. E.; LeFloch-Perrennou, F.; Petillon, F. Y.; Keith, A. N.; Manojlovic-Muir, L.; Muir, K. W.; Sharp, D. W. A. *J. Chem. Soc., Chem. Commun.* **1979**, 410. (c) Davidson, J. L.; Shiralian, M.; Manojlovic-Muir, L.; Muir, K. W. *J. Chem. Soc., Dalton Trans.* **1984**, 2167. (d) Ashby, M. T.; Enemark, J. H. *Abstracts, XIth International Conference on Organometallic Chemistry, Pine Mountain, GA, Oct. 1983*, No. 115. (e) Ashby, M. T.; Enemark, J. H. *Abstracts, XIIth International Conference on Organometallic Chemistry, Vienna, Austria, Sept. 1985*, No. 65. (f) Ashby, M. T.; Enemark, J. H. *Organometallics* **1987**, *6*, 1318.



For  $\phi = 180^\circ$ , the orientation observed in the solid state structure of  $\text{CpFe}(\text{CO})_2\text{SC}_2\text{H}_5$ ,<sup>14</sup> the calculation predicts that the occupied metal  $a''$  orbital will mix with the  $\text{SH}^-$  sulfur  $3p_x$  lone pair to give a stabilized symmetric combination ( $\pi_{||}$ ) and a destabilized antisymmetric combination ( $\pi^*_{||}$ ). The latter is the HOMO and is primarily sulfur  $3p_x$  in character. The  $\pi_{\perp}$  molecular orbital is largely  $2a'$  in character for  $\phi = 180^\circ$  (vide supra). Other rotational orientations of the  $\text{SH}^-$  ligand result in a similar bonding description but with different combinations of the  $2a'$  and  $a''$  orbitals of  $\text{CpFe}(\text{CO})_2^+$  with the  $3p_x$  orbital of  $\text{SH}^-$ . Figure 1b,c illustrates how the composition of the HOMO's of **1** vary with  $\phi$ . It is interesting that the calculations predict virtually no total energy barrier to rotation about the Fe-S bond. This is in sharp contrast to the significant rotational barrier calculated for single-sided  $\pi$ -acceptor ligands (e.g. carbenes) bound to the  $\text{CpFe}(\text{CO})_2^+$  group.<sup>15a</sup> Topological phase diagrams of the  $\pi_{||}$  and  $\pi^*_{||}$  orbitals for  $\phi = 90^\circ$  are shown in Figure 2.

**Spectroscopic Studies.** The electronic structure of **1** may be experimentally investigated by gas-phase photoelectron spectroscopy (PES). The arenethiols  $\text{HSC}_6\text{H}_4\text{-}p\text{-Z}$  ( $Z = \text{OMe}$ ,  $\text{H}$ ,  $\text{Cl}$ ,  $\text{CF}_3$ ,  $\text{NO}_2$ ) were chosen for this study for two reasons. First, the arene analogues of **1** are thermally stable and reasonably volatile. Second, the arene substituent provides a convenient means for perturbing the electron density at sulfur. Electron-donating groups ( $Z = \text{OMe}$ ) should raise the energy of the antibonding orbital  $\pi^*_{||}$  and increase its separation from  $\pi_{||}$ . Strongly withdrawing substituents ( $Z = \text{NO}_2$ ) should stabilize the antibonding orbital ( $\pi^*_{||}$ ) by decreasing the electron density on the sulfur atom.

A prerequisite to assigning the PE spectra of **1** is assignment of the free thiolate ligand spectra. The PE spectrum of thiophenol is shown in Figure 3. Arenethiols have not been thoroughly investigated previously by PES, although the spectra of the other substituted benzenes have been extensively studied. The PE spectrum of thiophenol differs significantly from that of phenol because of the greater stability of the oxygen orbitals relative to those of sulfur. The first ionization energies of alkyl- and hydrosulfur compounds are actually more similar to those of corresponding nitrogen compounds,<sup>19</sup> and studies of the PE spectra of aniline and related compounds provide insight into the PE spectrum of thiophenol. The PE spectrum of aniline reveals three low-energy bands that have been assigned to the  $\pi_3$  ( $3b_1$ ),  $\pi_2$  ( $1a_2$ ), and nitrogen lone pair ( $2b_1$ ) (Figure 4).<sup>19</sup> Upon sequential substitution of the hydrogens bound to the nitrogen atom of aniline with more donating methyl groups, both the  $\pi_3$  and lone-pair bands are destabilized. In contrast, the  $\pi_2$  ( $1a_2$ ) orbital is practically unaffected by the substitutions. This indicates that the first ( $3b_1$ ) and third ( $2b_1$ ) ionizations result from two molecular orbitals that are an antisymmetric and a symmetric combination of the appropriate ring  $\pi$  and nitrogen lone-pair orbitals, respectively. The  $2b_1$  shifts slightly more than the  $3b_1$  orbital in the substituted analogues of aniline, which indicates the greater nitrogen character of the  $2b_1$  orbital.

A similar situation is observed for thiophenol. The first three ionization bands, an increasing order of stability, are attributed to the  $3b_1$ ,  $1a_2$ , and  $2b_1$  orbitals. The HOMO ionization for thiophenol ( $3b_1$ ) is expected to have greater heteroatom character as compared to that of aniline because of the more closely matched electronegativities of carbon and sulfur as compared to those of

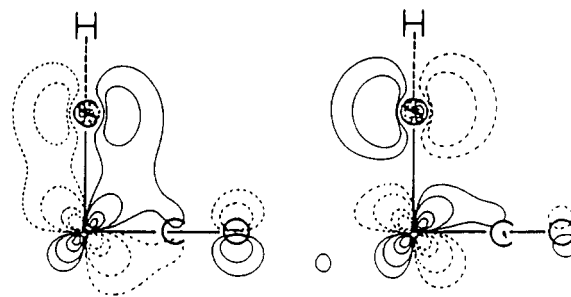


**Figure 2.** Topological phase diagrams for  $\pi_{||}$  (left) and  $\pi^*_{||}$  (right). A rotational angle of  $\phi = 90^\circ$  was chosen to simultaneously illustrate the  $\pi$ -donor orbital of the  $\text{SH}$  ligand and a  $\pi$ -acceptor orbital of the  $\text{CO}$  ligand. The outer contour lines correspond to a density of  $2^{-8} e^-/\text{au}^3$ , and each successive contour line value is related by a factor of 4.

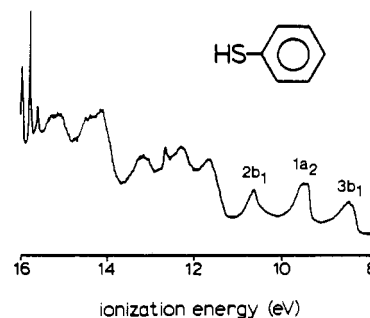


**Figure 3.** He I photoelectron spectrum of thiophenol.

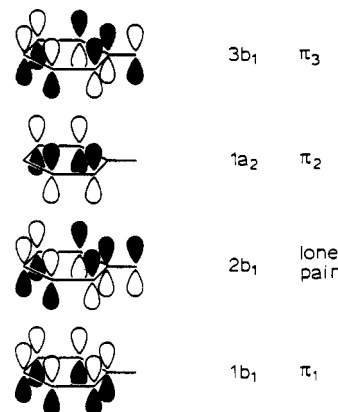


**Figure 4.** Symmetry labels for the  $\pi$ (aryl) and lone-pair orbitals of  $\text{C}_6\text{H}_5\text{X}$ .

**Table II.** Spectroscopic Properties for  $\text{CpFe}(\text{CO})_2\text{SC}_6\text{H}_4\text{-}p\text{-Z}$  and Its Reaction Rate with Iodomethane

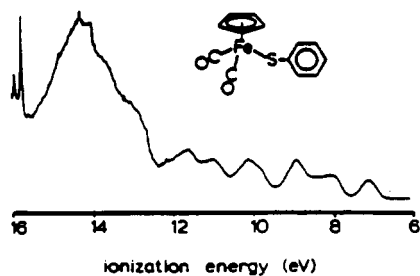
Z	$\nu_{\text{CO}}$ , <sup>a</sup> $\text{cm}^{-1}$	$\delta_{\text{Cp}}$ <sup>b</sup>	HOMO		
			IP, eV	$k_r$ , <sup>d</sup> $\text{L mol}^{-1} \text{s}^{-1}$	$k_{\text{rel}}$
OMe	2032, 1984	4.89	c	$6.8 (4) \times 10^{-3}$	107.9
H	2035, 1987	4.94	7.12	$1.55 (3) \times 10^{-3}$	25.4
Cl	2036, 1989	4.95	7.22	$6.5 (3) \times 10^{-4}$	10.3
$\text{CF}_3$	2039, 1992	5.01	7.31	$3.65 (3) \times 10^{-4}$	5.7
$\text{NO}_2$	2043, 1997	5.10	7.58	$6.3 (4) \times 10^{-5}$	1.0

<sup>a</sup> Obtained as  $\text{CHCl}_3$  solutions between  $\text{NaCl}$  plates. <sup>b</sup> Obtained as  $\text{CDCl}_3$  solutions. <sup>c</sup> PES could not be obtained; see text. <sup>d</sup> Reaction of  $\text{CpFe}(\text{CO})_2\text{SC}_6\text{H}_4\text{-}p\text{-Z}$  with iodomethane in acetone- $d_6$  at  $20^\circ\text{C}$ .

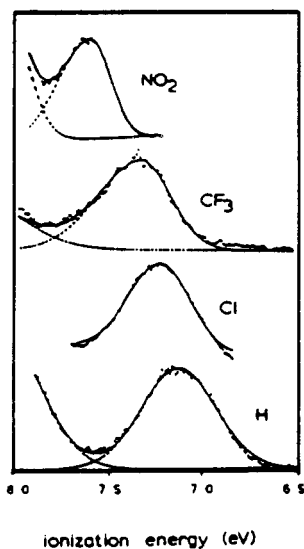
carbon and nitrogen. Furthermore, the sulfur lone pair and  $\pi$ (aryl) orbitals are expected to mix to a larger extent in thiophenol as compared to aniline due to the greater p character of the sulfur lone pair. The first ionization (8.46 eV) is of principal interest in this study, for this band corresponds to the only orbital with sulfur character that has the correct symmetry and is energetically favored to interact with metal  $d\pi$  orbitals.

The valence photoelectron spectrum of **1** ( $\text{R} = \text{C}_6\text{H}_5$ ) is shown in Figure 5a. The predominantly metal ionizations likely occur

(19) (a) Turner, D. W.; May, D. P. *J. Chem. Phys.* **1966**, *45*, 471. (b) Turner, D. W.; May, D. P. *Ibid.* **1967**, *46*, 1156. (c) Turner, D. W.; Baker, C.; Baker, A. D.; Brundle, C. R. *Molecular Photoelectron Spectroscopy*; Wiley-Interscience: New York, 1970; p 300. (d) Ebel, S.; Bergmann, H.; Ensslin, W. *J. Chem. Soc., Faraday Trans 2* **1974**, *70*, 555.



a



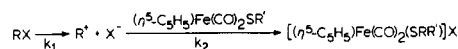
b

Figure 5. (a) Full He I photoelectron spectrum of  $\text{CpFe}(\text{CO})_2\text{SC}_6\text{H}_5$ . (b) Expanded He I photoelectron spectra of the HOMO ionization of  $\text{CpFe}(\text{CO})_2\text{SC}_6\text{H}_4\text{-}p\text{-Z}$ .

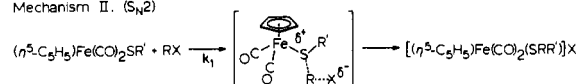
in the region of 8–9 eV in analogy with the ionizations of other  $\text{CpFe}(\text{CO})_2\text{X}$  complexes.<sup>20h</sup> The Cp,  $\pi$ (aryl), and substituent lone-pair orbitals of **1** ( $\text{R} = \text{C}_6\text{H}_4\text{-}p\text{-Z}$ ) give rise to additional ionization features at greater than 9 eV. Specific assignment of these features is not the focus of this work and is not attempted on the basis of the present data. The most significant results are related to the trends in the HOMO ionization potentials observed for **1** ( $\text{R} = \text{C}_6\text{H}_4\text{-}p\text{-Z}$ ;  $\text{Z} = \text{H}, \text{Cl}, \text{CF}_3, \text{NO}_2$ ) as shown in Figure 5b and summarized in Table II. In addition to the HOMO IP's, Table II also lists the carbonyl stretching frequencies and the  $^1\text{H}$  NMR cyclopentadienyl chemical shifts. The HOMO IP decreases in binding energy, the carbonyl stretching frequencies decrease, and the shielding of the cyclopentadienyl protons increases as Z becomes a better donor.<sup>20</sup>

If Fenske–Hall calculations correctly predict the HOMO of **1** to be metal–sulfur antibonding and principally sulfur in character, then the PE spectra indicate the thiolate  $3b_1$  orbital has been destabilized relative to thiophenol by ca. 1.3 eV. This destabilization is the result of two cooperating effects, the Coulombic (charge) difference between hydrogen and the  $\text{CpFe}(\text{CO})_2$  fragment and filled–filled interactions between the sulfur 3p lone

Mechanism I. ( $\text{S}_{\text{N}}1$ )



Mechanism II. ( $\text{S}_{\text{N}}2$ )



Mechanism III. (electron transfer)

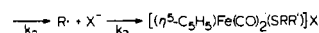
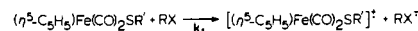


Figure 6. Possible mechanisms for the reaction of  $\text{CpFe}(\text{CO})_2\text{SR}$  and alkyl halides.

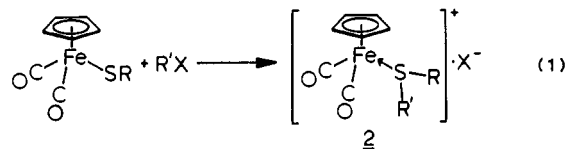
Table III. Effect of the Iodoalkane on the Reaction Rate<sup>a</sup>

iodoalkane	$k$ , $\text{L mol}^{-1} \text{s}^{-1}$	$k_{\text{rel}}$
$\text{ICH}_3$	$1.55 (3) \times 10^{-3}$	18.0
$\text{ICH}_2\text{CH}_3$	$8.6 (2) \times 10^{-5}$	1.0
$\text{ICH}(\text{CH}_3)_2$	no reaction	
$\text{IC}(\text{CH}_3)_3$	no reaction	

<sup>a</sup> Reaction of the iodoalkane with  $\text{CpFe}(\text{CO})_2\text{SC}_6\text{H}_5$  in acetone- $d_6$  at 20 °C.

pair and occupied iron  $d\pi$  orbitals. The observed substituent effect on the HOMO ionization potential, the carbonyl stretching frequencies, and the cyclopentadienyl  $^1\text{H}$  NMR chemical shifts indicate the presence of  $d\pi\text{-}p\pi$  antibonding orbital interactions between the thiolate ligand and the metal.

**Reactivity Studies.** The mixing of the thiolate 3p lone pair with the metal  $d\pi$  orbitals should influence the reactivity of **1** with electrophiles. Such a reaction has been reported by King et al. in which **1** ( $\text{R} = \text{CH}_3$ ) was treated with iodomethane to give the salt  $[\text{CpFe}(\text{CO})_2(\text{S}(\text{R})(\text{R}'))]^+ \text{I}^-$ , **2** ( $\text{R} = \text{R}' = \text{CH}_3$ ):<sup>21</sup>



Compound **1** ( $\text{R} = \text{C}_6\text{H}_4\text{-}p\text{-Z}$ ;  $\text{Z} = \text{OMe}, \text{H}, \text{Cl}, \text{CF}_3, \text{NO}_2$ ) also reacts with iodomethane in polar solvents at room temperature to give the corresponding thioether complex **2** ( $\text{R} = \text{C}_6\text{H}_4\text{-}p\text{-Z}$ ;  $\text{Z} = \text{OMe}, \text{H}, \text{Cl}, \text{CF}_3, \text{NO}_2$ ;  $\text{R}' = \text{CH}_3$ ), which under more vigorous conditions undergoes nucleophilic substitution by the iodide anion to give the free thioether and  $\text{CpFe}(\text{CO})_2\text{I}$ . At room temperature the latter reaction is much slower than the former, and consequently, a rate constant for the reaction of **1** with iodomethane may be obtained by following the cyclopentadienyl resonance with  $^1\text{H}$  NMR spectroscopy.

Three plausible mechanisms were considered in interpreting the kinetic results from reaction 1 (Figure 6). Mechanism I involves an  $\text{S}_{\text{N}}1$ -like preionization of the alkyl halide followed by reaction of the resulting carbonium ion with the thiolate ligand of **1**. In mechanism II the halide is displaced by the thiolate ligand by way of a  $\text{S}_{\text{N}}2$ -like transition state. Mechanism III entails electron transfer from **1** to the alkyl halide. Many organo–thiolate reactions are known to proceed by way of an electron-transfer mechanism,<sup>22a</sup> and 17-electron cation-radical species of the type  $[\text{CpFe}(\text{CO})_2\text{SR}]^+$  (**3**) may be prepared chemically (reaction 3).<sup>23</sup>

The influence of the thiolate ligand substituent Z on the reaction rate is summarized in Table II. A correlation is observed between

- (20) (a) Nesmeyanov, A. N.; Chapovskii, Y. A.; Denisovich, L. I.; Lokshin, V. B.; Polovnyanyuk, I. V. *Dokl. Akad. Nauk. SSSR* **1967**, *174*, 1342. (b) Ugo, R.; Cenini, S.; Banati, F. *Inorg. Chim. Acta* **1967**, *1*, 451. (c) King, R. B. *Inorg. Chim. Acta* **1968**, *2*, 454. (d) Dalton, J.; Paul, I.; Stone, F. G. A. *J. Chem. Soc. A* **1969**, 2744. (e) Darenbourg, D. J. *Inorg. Chem.* **1972**, *11*, 1606. (f) Nesmeyanov, A. N.; Leshcheva, I. F.; Iovanyuk, I. V.; Ustynuk, Y. A.; Mararova, L. G. *J. Organomet. Chem.* **1972**, *37*, 159. (g) Symon, D. A.; Waddington, T. C. *J. Chem. Soc., Dalton Trans.* **1975**, 2140. (h) Lichtenberger, D. L.; Fenske, R. F. *J. Am. Chem. Soc.* **1976**, *98*, 50.

- (21) King, R. B.; Bisnette, M. B. *Inorg. Chem.* **1965**, *4*, 482.  
 (22) Cary, F. A.; Sunberg, R. J. *Advanced Organic Chemistry, Part A*; Plenum: New York, 1980: (a) p 548; (b) p 146.  
 (23) (a) Treichel, P. M.; Rosenhein, L. D.; Schmidt, M. S. *Inorg. Chem.* **1983**, *22*, 3960. (b) Treichel, P. M.; Rosenhein, L. D. *Inorg. Chem.* **1984**, *23*, 4018.

**Table IV.** Effect of Solvent Polarity on the Reaction Rate<sup>a</sup>

solvent	$k$ , L mol <sup>-1</sup> s <sup>-1</sup>	$k_{rel}$
dimethyl- <i>d</i> <sub>6</sub> sulfoxide	$1.65 (4) \times 10^{-2}$	12.1
acetone- <i>d</i> <sub>6</sub>	$1.55 (3) \times 10^{-3}$	1.1
chloroform- <i>d</i> <sub>1</sub>	$1.37 (4) \times 10^{-3}$	1.0

<sup>a</sup> Reaction of CpFe(CO)<sub>2</sub>SC<sub>6</sub>H<sub>5</sub> with iodomethane in the given solvent at 20 °C.

the relative donor ability of the aryl substituent and reaction rate. In fact, a linear free energy relationship is observed between the reaction rate and the Hammett substituent constant. The calculated Hammett reaction constant ( $\rho = -1.82$ ) suggests a developing positive charge on sulfur prior to the rate determining step in reaction 1.<sup>22b</sup> This result is most consistent with mechanism II.

The effect of the alkyl halide on the reaction rate (ICH<sub>3</sub> > ICH<sub>2</sub>CH<sub>3</sub> >> ICH(CH<sub>3</sub>)<sub>2</sub> = IC(CH<sub>3</sub>)<sub>3</sub> = 0) is inconsistent with mechanisms I and III as both carbonium and radical species are stabilized by the additional donor and/or steric influence of the more substituted alkyl halides (Table III).<sup>24a</sup> A dependence on the halide was qualitatively observed (e.g. iodides would often react when the analogous bromide and chloride would not), but this latter observation does not lend support to any of the mechanisms in particular.<sup>24b</sup>

The dependence of the reaction rate for reaction 1 on solvent polarity (Table IV) is consistent with the developing charges in mechanism I and II.<sup>24c</sup>

Several experiments designed to detect or trap radical species were conducted; however, the results were all negative. No evidence for a CIDNP effect was observed in the <sup>1</sup>H NMR spectrum of the reaction mixture.<sup>25</sup> Furthermore, radical species were not observed in the EPR spectra, even in the presence of the radical trap 2-methyl-2-nitrosopropane dimer.<sup>26</sup> Cyclizable primary alkyl halides have been used in other studies as mechanistic probes to distinguish between S<sub>N</sub>2 and electron-transfer processes.<sup>27</sup> One such reagent is 6-bromo-1-hexene.<sup>28</sup> Unfortunately neither 6-bromo- nor 6-iodo-1-hexene react with **1** (R = C<sub>6</sub>H<sub>5</sub>). However, 6-iodo-1-hexene reacts cleanly in DMSO with the more nucleophilic **1** (R = C<sub>2</sub>H<sub>5</sub>) to first yield **2** (R = C<sub>2</sub>H<sub>5</sub>, R' = (CH<sub>2</sub>)<sub>4</sub>CH=CH<sub>2</sub>) which further reacts to give CpFe(CO)<sub>2</sub>I and free 6-(ethylthio)-1-hexene.

Although these experiments individually do not prove that mechanism III is incorrect, together they indicate that radical species are not involved. Therefore, we conclude that mechanism II is the likely pathway for the reaction of **1** with alkyl halides.

The reaction of **1** with iodomethane exhibits a substantial substituent effect that spans several orders of magnitude. Figure 7 demonstrates the Hammett relationship between the rate of nucleophilic attack of **1** on iodomethane and the spectroscopic properties given in Table II. The observed correlation between the HOMO IP of **1** and the reaction rate lends credence to our assignment of the HOMO of **1** as substantially sulfur lone pair in character. Furthermore, the correlation between the carbonyl stretching frequencies and the cyclopentadienyl ligand <sup>1</sup>H NMR chemical shifts and the reaction rate is evidence for an interaction of the sulfur lone pair with the metal orbitals.

Clearly, an enhanced nucleophilicity at sulfur is evidenced by the reactivity of **1** toward alkyl halides (reaction 1), a reaction that is not generally observed for thiolate ligands bound to high-valent and/or electron-poor metals. Reaction 1 illustrates

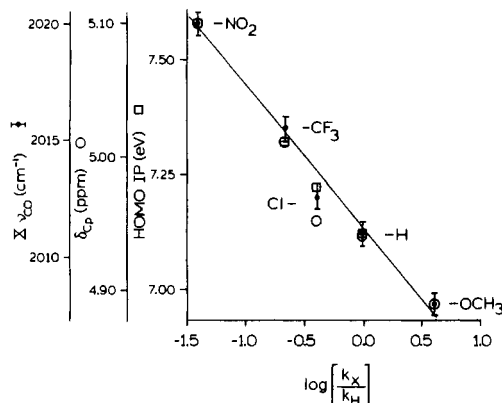
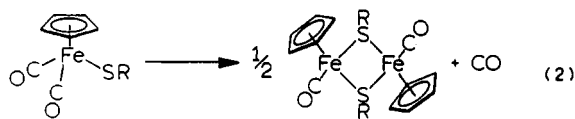


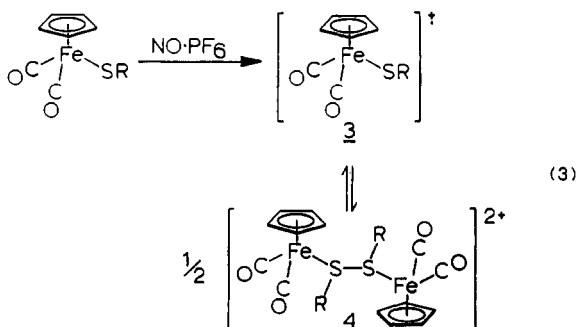
**Figure 7.** Hammett relationships between the rate of reaction of CpFe(CO)<sub>2</sub>SC<sub>6</sub>H<sub>4</sub>-*p*-Z with iodomethane and the spectroscopic properties for CpFe(CO)<sub>2</sub>SC<sub>6</sub>H<sub>4</sub>-*p*-Z listed in Table II.

the influence of filled metal–filled sulfur orbital interactions on the stability of **1**. The filled–filled interaction can also explain the propensity of **1** to dimerize with loss of CO:<sup>9</sup>



It has been shown previously that  $\pi$ -donor ligands labilize cis carbonyls for dissociation from d<sup>6</sup> metal centers.<sup>30</sup> The instability and high sulfur character of the antibonding orbital combination (Figure 1,  $\pi^*_{||}$ ) also favors donation from this orbital to a neighboring metal complex and will contribute to the relative stability of the dimer species. Reaction 2 is more prevalent for **1** (R = alkyl) than **1** (R = aryl), which may be attributed to the greater donor ability of alkyl as compared to aryl groups.

Compound **1** undergoes additional unique chemistry that deserves particular attention. For example, a novel dimerization reaction has been observed when **1** is oxidized by one electron:<sup>23</sup>



The 17-electron complex **3** is of immediate relevance since the orbital from which the electron has been removed is the iron–sulfur  $\pi$ -antibonding HOMO ( $\pi^*_{||}$ ). We have conducted an open-shell Fenske–Hall molecular orbital calculation on **3** (R = H) and have found the results quite similar to those obtained for **1** (R = H); that is,  $\pi^*_{||}$  is still largely sulfur in character but only half-occupied.<sup>16</sup> This may also explain why the equilibrium for reaction 3 generally lies toward the diamagnetic species **4**. The dimerization of **3** serves to reduce the filled–filled orbital interactions. What is somewhat surprising is that dimerization is less favored when the carbonyl ligands on **3** are replaced with electron-donating ligands (e.g. phosphines). Furthermore, when the carbonyl ligands are replaced with CNC<sub>6</sub>H<sub>4</sub>-*m*-OMe and CNC<sub>6</sub>H<sub>4</sub>-*m*-CF<sub>3</sub> the more electron-withdrawing isocyanide (CNC<sub>6</sub>H<sub>4</sub>-*m*-CF<sub>3</sub>) favors dimerization to a greater degree. This result at first seems unexpected. It has been postulated that the occupied iron  $d\pi$  orbitals in **4** donate to the sulfur–sulfur  $\sigma^*$  orbital.<sup>23b</sup> Although

(24) (a) March, J. *Advanced Organic Chemistry*; McGraw-Hill: New York, 1977: (a) p 315; (b) p 322; (c) p 331.

(25) Lepley, C. *Chemically Induced Magnetic Polarization*; Wiley: New York, 1973.

(26) Janzen, E. G. *Acc. Chem. Res.* **1974**, *4*, 31.

(27) Ashby, E. C.; Su, W.; Pham, T. N. *Organometallics* **1985**, *4*, 1493 and references contained therein.

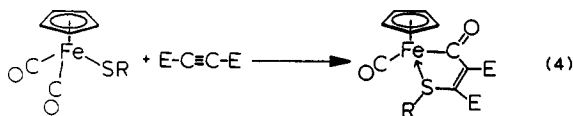
(28) 6-Halo-1-hexenes may not be the most effective cyclizable primary halide.<sup>27,29</sup>

(29) (a) Ashby, E. C., personal communication. (b) Ashby, E. C.; Pham, T.; Park, B.; Su, W. *Abstracts*, XIIth International Conference on Organometallic Chemistry, Vienna, Austria, Sept. 1985; No. 206.

(30) Lichtenberger, D. L.; Brown, T. L. *J. Am. Chem. Soc.* **1978**, *100*, 366.

we have not conducted a study of **4**, the calculations on **1** and **3** suggest an alternative explanation. The more electron-withdrawing isocyanide ligand lowers the energy of the metal  $d\pi$  orbitals, thereby decreasing the metal character and correspondingly increasing the sulfur character in the iron-sulfur  $\pi$ -antibonding HOMO ( $\pi^*$ ). This would tend to favor S-S bond formation to give the dimeric product **4**.

Another reaction of interest is the cycloaddition of electron-deficient alkynes to **1** to give a five-member heterometalacycle.<sup>18</sup>



This reaction is interesting in that the addition of the alkyne takes place at two different types of ligands, a  $\pi$  acceptor (carbonyl) and a  $\pi$  donor (thiolate). The mechanism of this novel  $[4\pi + 2\pi]$  cycloaddition reaction has been previously discussed.<sup>18f</sup>

### Conclusions

Fenske-Hall molecular orbital calculations on **1** ( $R = H$ ) predict a  $d\pi$ - $p\pi$  orbital interaction between the formally occupied  $d\pi$  iron orbitals and the lone pair on sulfur that is principally  $3p$  in character. This interaction results in a destabilized antibonding combination that is the highest occupied molecular orbital and principally sulfur  $3p$  in character. The results of the calculations are supported by spectroscopic studies including photoelectron spectra for **1** ( $R = C_6H_4$ - $p$ - $Z$ ;  $Z = OMe, H, Cl, CF_3, NO_2$ ) which reveal an energetically isolated high-energy band that shows a significant substituent effect. These spectroscopic results correlate with the kinetic results obtained from the reaction of **1** and alkyl halides. Mechanistic studies of this reaction support an  $S_N2$ -type nucleophilic displacement of the halide by the coordinated thiolate

ligand. The correlation of the spectroscopic and kinetic results lends additional support to our postulate that the HOMO of **1** is principally sulfur in character. We conclude that the enhanced nucleophilicity of the sulfur atom of **1** is due to a destabilizing filled-filled  $d\pi$ - $p\pi$  orbital interaction between the  $p$ -type sulfur lone pair and the formally occupied metal  $d\pi$  orbitals. These results contrast with the stabilizing filled-empty  $d\pi$ - $p\pi$  orbital interactions observed for  $CpMo(NO)(SR)_2$ .<sup>4d</sup>

**Acknowledgment.** We wish to thank Dr. K. Christensen for assistance with the NMR experiments, Dr. G. E. Kellogg for assistance with the PES experiments carried out in the Laboratory for Electron Spectroscopy and Surface Analysis, and Prof. R. S. Glass for valuable discussion. Financial support of this work by the National Institute of Environmental Health Sciences (Grant ES 00966) (J.H.E.), the Department of Energy (Division of Chemical Sciences, Office of Basic Energy Sciences, Office of Energy Research, Grant DE-AC02-80ER10746) (D.L.L.), and the Materials Characterization Program, Department of Chemistry, University of Arizona, is gratefully acknowledged. In addition, M.T.A. thanks the University of Arizona Summer Research Support Program for their award of a research assistantship.

**Registry No.** **1** ( $R = C_6H_4$ - $p$ - $OMe$ ), 110935-19-8; **1** ( $R = C_6H_5$ ), 12110-44-0; **1** ( $R = C_6H_4$ - $p$ - $Cl$ ), 110935-20-1; **1** ( $R = C_6H_4$ - $p$ - $CF_3$ ), 110935-21-2; **1** ( $R = C_6H_4$ - $p$ - $NO_2$ ), 110935-22-3; **1** ( $R = C_2H_5$ ), 12108-34-8; **1** ( $R = H$ ), 110935-18-7; **2** ( $R = C_2H_5$ ,  $R' = (CH_2)_6CH=CH_2$ ,  $X = I$ ), 110935-23-4; **2** ( $R = C_6H_4$ - $p$ - $OMe$ ,  $R' = Me$ ,  $X = I$ ), 110935-24-5; **2** ( $R = C_6H_5$ ,  $R' = Me$ ,  $X = I$ ), 110935-25-6; **2** ( $R = C_6H_4$ - $p$ - $Cl$ ,  $R' = Me$ ,  $X = I$ ), 110935-26-7; **2** ( $R = C_6H_4$ - $p$ - $CF_3$ ,  $R' = Me$ ,  $X = I$ ), 110935-27-8; **2** ( $R = C_6H_4$ - $p$ - $NO_2$ ,  $R' = Me$ ,  $X = I$ ), 110935-28-9; **3** ( $R = H$ ), 110935-29-0;  $HSC_6H_4$ - $p$ - $OMe$ , 696-63-9;  $HSC_6H_5$ , 108-98-5;  $HSC_6H_4$ - $p$ - $Cl$ , 106-54-7;  $HSC_6H_4$ - $p$ - $CF_3$ , 825-83-2;  $HSC_6H_4$ - $p$ - $NO_2$ , 1849-36-1;  $CpFe(CO)_2I$ , 12078-28-3;  $HS(CH_2)_4CH=CH_2$ , 18922-04-8; 6-iodo-1-hexene, 2695-47-8; 6-(ethylthio)-1-hexene, 75199-72-3.

## Notes

Contribution from the Department of Chemistry,  
University of California at Santa Barbara,  
Santa Barbara, California 93106

### Oxygen Transfer from *p*-Cyano-*N,N*-dimethylaniline *N*-Oxide to the $\mu$ -Oxo Dimer of (*meso*-Tetraphenylporphinato)iron(III)

C. Michael Dicken, P. N. Balasubramanian,  
and Thomas C. Bruice\*

Received June 22, 1987

Dealkylation of tertiary amines in hepatic microsomes is carried out on reaction with the NADH/O<sub>2</sub> cytochrome P-450 enzymes and via flavin mixed-function oxidase conversion of the primary amine to an *N*-oxide, which then reacts with a cytochrome P-450 enzyme in a reaction that does not require NADH nor O<sub>2</sub>.<sup>1,2</sup> The mechanisms of reaction of *N*-oxides with iron(III) porphyrins is of considerable interest.<sup>3-9</sup> In this investigation we examine the

reaction of the  $\mu$ -oxo dimer of (*meso*-tetraphenylporphinato)iron(III) ( $((TPP)Fe^{III})_2O$ ) with *p*-cyano-*N,N*-dimethylaniline *N*-oxide (DAO). Our objectives have been to probe the reactions that proceed from the immediate higher valent product of oxygen transfer to the  $\mu$ -oxo dimer (i.e.,  $(TPP)Fe^{III}O-Fe^{IV}(O)(TPP^{+})$ ).

### Methods and Materials

The  $\mu$ -oxo dimer of (*meso*-tetraphenylporphinato)iron(III) ( $(TPP)Fe^{III})_2O$ ) was synthesized by the method of Kobayashi and co-workers<sup>10</sup> and characterized by its UV-vis spectra. *p*-Cyano-*N,N*-dimethylaniline *N*-oxide (DAO) was prepared as given elsewhere.<sup>11</sup> The sources of all other chemicals used in this study have been reported.<sup>5</sup>

### Results

In this investigation, the reaction of *p*-cyano-*N,N*-dimethylaniline *N*-oxide (DAO) with the  $\mu$ -oxo dimer of (*meso*-tetraphenylporphinato)iron(III) ( $((TPP)Fe^{III})_2O$ ) has been studied in grade A<sup>5</sup> CH<sub>2</sub>Cl<sub>2</sub> solvent (at 25 °C under N<sub>2</sub>). The products of decomposition of DAO are *p*-cyano-*N,N*-dimethylaniline (DA), *p*-cyano-*N*-methylaniline (MA), *p*-cyanoaniline (A), *p*-cyano-*N*-formyl-*N*-methylaniline (FA), *N,N'*-dimethyl-*N,N'*-bis(*p*-cyanophenyl)hydrazine (H), and *N,N'*-bis(*p*-cyanophenyl)-*N*-methylmethylenediamine (MD). Products with time were monitored at 320 nm, where absorption by the metalloporphyrin is minimal. Yields by HPLC analysis at 280 and 320 nm (based upon [DAO]<sub>i</sub>): DA, 59%; MA, 18%; A, 3%; FA, 6%; H, 8%; MD, 7%; all at [DAO]<sub>i</sub>/[( $(TPP)Fe^{III})_2O$ ]<sub>i</sub> ratios of 10-100. The yield of

- White, R. E.; Coon, M. J. *Annu. Rev. Biochem.* **1980**, *49*, 315.
- Hamill, S.; Cooper, D. Y. *Xenobiotica* **1984**, *14*, 139.
- Shannon, P.; Bruice, T. C. *J. Am. Chem. Soc.* **1981**, *103*, 4580.
- Nee, M. W.; Bruice, T. C. *J. Am. Chem. Soc.* **1982**, *104*, 6123.
- Dicken, C. M.; Lu, F.-L.; Nee, M. W.; Bruice, T. C. *J. Am. Chem. Soc.* **1985**, *107*, 5776.
- Dicken, C. M.; Woon, T. C.; Bruice, T. C. *J. Am. Chem. Soc.* **1986**, *108*, 1636.
- Woon, T. C.; Dicken, C. M.; Bruice, T. C. *J. Am. Chem. Soc.* **1986**, *108*, 7990.
- Bruice, T. C.; Dicken, C. M.; Balasubramanian, P. N.; Woon, T. C.; Lu, F.-L. *J. Am. Chem. Soc.* **1987**, *109*, 3436.
- Ostovic, D.; Knobler, C. B.; Bruice, T. C. *J. Am. Chem. Soc.* **1987**, *109*, 3444.
- Kobayashi, H.; Higuchi, T.; Kaizu, Y.; Osada, H.; Aoki, M. *Bull. Chem. Soc. Jpn.* **1975**, *48*, 3137.
- Craig, J. C.; Purushothman, K. K. *J. Org. Chem.* **1970**, *35*, 1721.